Received: 29 October 2020 | Revised: 14 April 2021 | Accepted: 21 April 2021

DOI: 10.1111/ejn.15256

SPECIAL ISSUE ARTICLE

EJN European Journal of Neuroscience FENS WILEY

Disarranged neuroplastin environment upon aging and chronic stress recovery in female Sprague Dawley rats

Marta Balog[1] | **Senka Blažetić**[2] | **Vedrana Ivić**[1] | **Irena Labak**[2] | **Bartosz Krajnik**[3] | **Raquel Marin**[4] | **Ana Canerina-Amaro**[4] | **Daniel Pereda de Pablo**[4] | **Ana Bardak**[1] | **Robert Gaspar**[5] | **Kálmán Ferenc Szűcs**[5] | **Sandor G. Vari**[6] | **Marija Heffer**[1]

[1]Department of Medical Biology and Genetics, Faculty of Medicine, J. J. Strossmayer University of Osijek, Osijek, Croatia

[2]Department of Biology, J. J. Strossmayer University of Osijek, Osijek, Croatia

[3]Department of Experimental Physics, Wroclaw University of Science and Technology, Wroclaw, Poland

[4]Laboratory of Cellular Neurobiology, Department of Basic Medical Sciences, School of Health Sciences, Universidad de La Laguna, La Laguna, Spain

[5]Department of Pharmacology and Pharmacotherapy, Faculty of Medicine, Interdisciplinary Excellence Centre, University of Szeged, Szeged, Hungary

[6]Cedars-Sinai Medical Center, International Research and Innovation in Medicine Program, Los Angeles, CA, USA

Correspondence
Marija Heffer, Department of Medical Biology and Genetics, Faculty of Medicine, J. J. Strossmayer University of Osijek, J. Huttlera 4, 31000 Osijek, Croatia.
Email: mheffer@mefos.hr

Funding information
Hungarian Ministry of Human Capacities, Grant/Award Number: 20391-3/2018/FEKUSTRAT; European Union through the European Regional Development Fund, Operational Programme Competitiveness, and Cohesion, Grant/Award Number: KK.01.1.1.01.0007; Spanish Ministry of Science and Innovation; European Union through the European Regional Development Fund, Grant/Award Number: SAF2017-85554-R; Cedars-Sinai Medical Center's International Research and Innovation in Medicine Program and RECOOP HST Association; Erasmus; Croatian Science Foundation, Grant/Award Number: IP-2014-09-2324; Cedars-Sinai Medical Center's International Research and Innovation in Medicine Program and

Abstract

Chronic stress produces long-term metabolic changes throughout the superfamily of nuclear receptors, potentially causing various pathologies. Sex hormones modulate the stress response and generate a sex-specific age-dependent metabolic imprint, especially distinct in the reproductive senescence of females. We monitored chronic stress recovery in two age groups of female Sprague Dawley rats to determine whether stress and/or aging structurally changed the glycolipid microenvironment, a milieu playing an important role in cognitive functions. Old females experienced memory impairment even at basal conditions, which was additionally amplified by stress. On the other hand, the memory of young females was not disrupted. Stress recovery was followed by a microglial decrease and an increase in astrocyte count in the hippocampal immune system. Since dysfunction of the brain immune system could contribute to disturbed synaptogenesis, we analyzed neuroplastin expression and the lipid environment. Neuroplastin microenvironments were explored by analyzing immunofluorescent stainings using a newly developed Python script method. Stress reorganized glycolipid microenvironment in the *Cornu Ammonis 1* (CA1) and dentate gyrus (DG) hippocampal regions of old females but in a very different fashion, thus affecting neuroplasticity. The postulation of four possible neuroplastin environments pointed to the GD1a ganglioside enrichment during reproductive

Abbreviations: AD, Alzheimer's disease; AMPA-R, α-amino-3-hydroxy-5-methyl-4-isoxazolepropionic acid receptor; APP, amyloid precursor protein; Aβ, amyloid beta; BACE1, beta-secretase 1; CA1, *Cornu Ammonis* subfield 1; CA2, *Cornu Ammonis* subfield 2; DG, dentate gyrus; GFAP, glial fibrillary acidic protein; HPA, hypothalamic-pituitary-adrenal axis; Iba1, ionized calcium binding adaptor molecule 1; IDV, integrated density value; Np65, neuroplastin.

Edited by: Mathias Schmidt

This is an open access article under the terms of the Creative Commons Attribution-NonCommercial-NoDerivs License, which permits use and distribution in any medium, provided the original work is properly cited, the use is non-commercial and no modifications or adaptations are made.
© 2021 The Authors. European Journal of Neuroscience published by Federation of European Neuroscience Societies and John Wiley & Sons Ltd

the Association for Regional Cooperation in the Fields of Health, Science and Technology; Cedars-Sinai Medical Center's International Research and Innovation in Medicine Program and the RECOOP HST Association

senescence of stressed females, as well as its high dispersion in both regions and to GD1a and GM1 loss in the CA1 region. A specific lipid environment might influence neuroplastin functionality and underlie synaptic dysfunction triggered by a combination of aging and chronic stress.

KEYWORDS

GD1a, GM1, hippocampus, neurodegeneration, neuroinflammation, reproductive senescence

1 | INTRODUCTION

An increasing body of data has demonstrated that chronic stress may underlie various events leading to cellular senescence and cognitive impairment (Bussian et al., 2018; Kim & Diamond, 2002; Kuipers et al., 2003; Lyons & Bartolomucci, 2020; Sandi, 2004; Zhang et al., 2019), possibly contributing to Alzheimer's disease (AD) development. This hypothesis on the contribution of chronic stress to AD development is supported by the following observations: (a) preferential glucocorticoid receptor accumulates in the brain areas that are most damaged in AD (Soontornniyomkij et al., 2010); (b) both of the proteins involved in amyloid beta processing, amyloid precursor protein (APP), and beta-secretase 1 (BACE1) contain a glucocorticoid response element in their sequences (Lahiri, 2004; Sambamurti et al., 2004; Li et al., 2011); and (c) prednisone therapy in AD patients accelerated cognitive deterioration (Aisen et al., 2000). Chronic stress effects in the brain are potentiated by aging through a decrease in the number of neurons, brain volume shrinkage, neuronal networks changes, circadian rhythms disruption, and lipid profile changes (Hung et al., 2010; Williamson & Lyons, 2018). On the other hand, stress response is attenuated by estrogen; hence, estrogen deficiency causes stress-induced damage during aging. This damage is particularly evident in women, suggesting the existence of a sex-specific mechanism of neurodegeneration (Dumas et al., 2012; Falconi et al., 2016; Marin & Diaz, 2018; Zárate et al., 2017). In female Sprague Dawley rats, reproductive senescence starts at 8–10 months of age and is characterized by a decreased number of developing follicles and changes in estrous cyclicity (Cruz et al., 2017).

Another crucial factor contributing to brain preservation is related to cerebral lipid composition and homeostasis. Glycosphingolipids, especially gangliosides (sialic acid-containing glycosphingolipids) maintain the structure, function, and transport to target membranes of at least 10% of transmembrane proteins (Simons & Toomre, 2000). Ganglioside species are specifically abundant in the synaptic membranes (Blennow et al., 1991), a fact suggesting their involvement in synaptic processes. The four most common gangliosides in the adult brain are GD1a, GD1b, GT1b, and GM1 (Vajn et al., 2013).

Some of the proteins essential for synaptic plasticity regulation and memory formation are located specifically in lipid rafts (Beesley et al., 2014; Marin & Diaz, 2018; Prendergast et al., 2014). Neuroplastin is a raft-dependent protein belonging to the immunoglobulin superfamily. It is highly expressed in the hippocampus, where it regulates synaptic plasticity. The stability of this protein and its functioning within the neuronal membrane have been associated with GM1-enriched lipid rafts (Beesley et al., 2014; Marzban et al., 2003). Neuroplastin contributes to neurite growth, maintenance of excitatory, and inhibitory synapse ratio and mechanisms of long-term potentiation (Owczarek et al., 2011; Smalla et al., 2000). Neuroplastin knock-out mice ($Np^{-/-}$ mice) have a significantly disturbed hypothalamic-pituitary-adrenal (HPA) axis, as reflected in the increased concentration of serum corticosterone under basal conditions. Interestingly, they also display decreased locomotion and contextual memory (Beesley et al., 2014; Bhattacharya et al., 2017). These physiological anomalies have been shown to be sex-related, as males have a doubled corticosterone increase compared with females. Another molecule associated with lipid rafts is AMPA-R which mediates most of the excitatory synaptic transmission (Carter et al., 2004; Chang et al., 2006; Zhang et al., 2018). AMPA-R-mediated excitatory synaptic transmission in the hippocampus is decreased by chronic stress (Carter et al., 2004; Chang et al., 2006; Kallarackal et al., 2013; Zhang et al., 2018), while AMPA-R exocytosis and expression on the cell surface are decreased by the disruption of lipid rafts (Hou et al., 2008; Prendergast et al., 2014).

Aging significantly changes lipid raft matrix stability, a process associated with the development of AD (Díaz et al., 2018; Mesa-Herrera et al., 2019). GM1 ganglioside accumulation and GD1a decrease, especially in the hippocampus, were detected in AD (Mesa-Herrera et al., 2019; Svennerholm, 1994). However, it remains unclear whether the long-term stress exposure could intensify gangliosides loss and whether this process is sex-specific.

The hypothesis of this study is that chronic stress during aging in females structurally changes the lipid microenvironment, a milieu playing an important role in cognitive functions. Since lipid microdomains affect the synaptic plasticity and cognitive processes, the impairment of lipid microenvironment upon stress may act as a basis for early

neurodegeneration in a sex-specific manner. Here, we explored the impact of chronic stress on memory and brain preservation after chronic stress recovery in young and old female rats. Since several factors affect luminescence intensity, pixel intensities of immunofluorescent stainings were analyzed using a newly developed Python script in order to explore neuroplastin microenvironments in situ.

2 | MATERIALS AND METHODS

2.1 | Animals

The study was performed in 2016. Forty female Sprague Dawley rats (Charles River, Milano, Italy) were divided into four groups of 10 animals. This number of animals per group ensured adequate statistical power and was in compliance with the EU Directive on Animal Welfare. The animals were assigned to two age groups using simple Excel software randomization—young (3.5 months old) and old (12 months old) females, with appropriate control groups. The experiments with young females were performed at the Faculty of Medicine, J. J. Strossmayer University of Osijek, Croatia, and those with old females were performed at the Faculty of Pharmacy, University of Szeged, Hungary. Both series of experiments were carried out with the same equipment and chemicals, so they can be considered as a single experiment. The animals were housed in self-ventilating cages (EHRET, Freiburg, Germany), with five air changes per minute, stable room temperature (21 ± 2°C) and humidity (40%–60%). Standardized rat chow (Mucedola, Milan, Italy; cat. no: 4RF21) and tap water were always provided, except when overnight fasting was used as a stressor. The day cycle was set to 7.00 a.m. to 7.00 p.m. All experiments (except lights-on or noise during the night) were conducted in the morning or early afternoon (9.00 a.m. to 2.00 p.m.). The study was approved by the Ethics Committee of the Faculty of Medicine Osijek and Croatian Ministry of Agriculture under class: 602-04/14-08/06, number: 2158-61-07-14-118 and the National Scientific Ethics Committee on Animal Experimentation, Hungary (permission number: IV./3796/2015). The 3R principles and EU directive on laboratory animal welfare were strictly followed.

2.2 | Chronic stress protocol

The chronic stress protocol consisted of three 10-day stress cycles with the application of eight stressors (overnight light or noise exposure, rotation of the animals in cages on a laboratory shaker, forced swimming in cold water, restraint in metal tubes, insulin injection, exposure to cold, and overnight fasting) followed by a 14-day recovery period between each stress cycle (Figure 1). The protocol lasted for 10 weeks. Two different stressors were applied each day to avoid stressor-specific responses, with some stressors being applied multiple times during each stress cycle. In the control groups, sham stress was performed by handling the animals in the same way as animals in experimental groups, but the stressors were not applied in order to compensate for the stress arising from standard handling. The anesthetics use was not necessary since no physical pain was caused and no surgical procedures were performed. The tissues were collected 2 weeks after the last stress cycle to allow us to determine only the extended metabolic changes.

2.3 | Passive avoidance test

Memory impairment was assessed with a step-through passive avoidance test performed 1 day after the end of the third chronic stress cycle. The apparatus (Ugo Basile, Varese, Italy) delivered an electric shock through the steel grid floor. The parameters used were as follows: door delay for 10 s, 0.5 mA, a foot-shock for 2 s, and total cut-off time of 180 s. The test lasted for 3 days. On the first day, the animals were allowed to explore the device for 180 s with no shock applied. On the second day, each rat upon entering the dark compartment

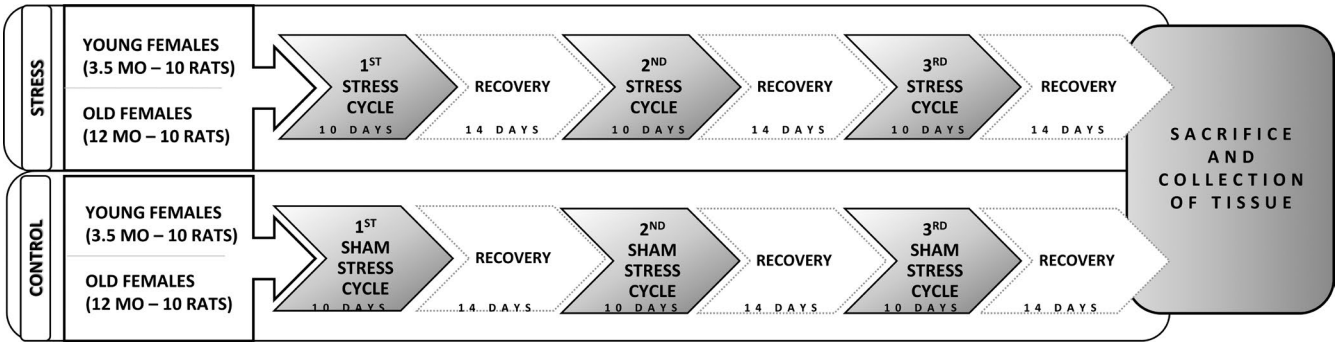

FIGURE 1 Chronic stress protocol scheme. Study included two experimental (stress) age groups ($N = 10$)—young (3.5 months old) and old (12 months old) female rats, with appropriate control groups (sham stress). The protocol lasted 10 weeks

received a foot-shock. On the third day, memory acquisition was recorded in terms of the total time (seconds) necessary for the animals to enter the dark compartment.

2.4 | Tissue collection

The animals were euthanized with isoflurane overdose (Forane® isofluranum, Abbott Laboratories LTD; Lake Bluff, IL, USA), which was applied in isoflurane induction chamber until loss of consciousness and combined with 30-mg/kg intramuscular ketamine injection (Ketanest, Pfizer Corporation, New York, NY, USA). The brains were isolated at the ages of 6 and 14.5 months, fixed in 4% buffered paraformaldehyde solution (pH = 7.35), cryoprotected in a series of sucrose solutions for 24 hr (10%, 20%, and 30% solutions) and cut using a cryostat (CM3050S, Leica, Nussloch, Germany) into 35-μm sagittal sections.

2.5 | Single immunohistochemical staining of AMPA-R, APP, microglia, and astrocytes

Single stainings were performed as previously described (Balog et al., 2015). The following primary and secondary antibodies were used: anti-ionized calcium-binding adapter molecule 1 (Iba1) (Wako, Neuss, Germany, cat. no: 019-19741) diluted to 1:1,000, antiglial fibrillary acidic protein (GFAP) (DAKO, Glostrup, Denmark, cat. no: M0761) diluted to 1:4,000, anti-AMPA-R subunit 2 (Neuro Mab, Davis, CA, USA, cat. no: L21/32) diluted to 1:500, biotinylated antimouse (Jackson Immunoresearch Laboratories, West Grove, PA, USA, cat. no: 115-065-166), byotinilated antigoat (Jackson Immunoresearch Laboratories, West Grove, PA, USA, cat no: 705-065-147), and byotinilated antirabbit (Jackson Immunoresearch Laboratories, West Grove, PA, USA, cat. no: 111-035-003) IgG antibodies combined with ABC kit (Vector Laboratories, CA, USA). All secondary antibodies were diluted to 1:500. The sections were mounted on glass slides and cover-slipped. In the case of fluorescent staining, primary anti-amyloid precursor protein (APP) (Abcam, Cambridge, UK, cat. no: ab32136) antibody was used (diluted to 1:1,000) in combination with CY3 antirabbit secondary antibody (Life Technologies, Carlsbad, CA, USA, cat. no: A10520). Peroxide pretreatment was omitted, and in the last step, the sections were incubated in 4′,6-diamidino-2-phenylindole (DAPI) diluted to a concentration of 1 μg/ml for 10 min at +4°C and rinsed again in PBS. The sections were mounted on microscope slides and cover-slipped. At 200× magnification, an area of 0.01 mm^2 of the *Cornu Ammonis* subfield 1 (CA1) and dentate gyrus (DG) hippocampal regions was imaged with an Olympus D70 camera (Olympus, Hamburg, Germany) set up on a Zeiss Axioskop 2 MOT microscope (Carl Zeiss Microscopy, Thornwood, NY, USA). In the case of fluorescent slides, the images were obtained with Olympus Fluoview FV1000 confocal microscope at 60× magnification, appropriate lasers and an Olympus FV10-ASW 4.2 Viewer software. The image resolution was 1,024 × 1,024 pixels.

2.6 | Triple immunofluorescent staining of neuroplastin, GD1a, and GM1 gangliosides

Free-floating sagittal brain sections were incubated in a blocking solution (1% BSA, 5% donkey serum, 5% goat serum) for 2 hr at +4°C followed by incubation for 48 hr at +4°C with two primary antibodies diluted in blocking solution: mouse anti-GD1a-1 (provided by prof. Schnaar, Johns Hopkins University, Baltimore, MA, USA, dilution 1:3,000) and goat antineuroplastin (Np65) (R&D Systems, Minneapolis, MN, USA, cat. no: AF5360, diluted 1:300). After four 10-min washes in PBS, the sections were incubated for 4 hr at +4°C with appropriate secondary antibodies: AF647 antimouse and CY3 antigoat (AF647 antimouse and CY3 antigoat; Jackson Immunoresearch Laboratories, West Grove, PA, USA, cat. no: 715-605-151 and 705-165-147, both diluted 1:500). After rinsing, the sections were additionally incubated (1.5 hr) with cholera toxin beta subunit conjugated with FITC fluorophore (Sigma, Saint Louis, MO, USA, cat. no: C1655, diluted 1:650) aimed to target GM1 ganglioside (referred to as GM1 later in the text to simplify the explanation of the results). Cholera toxin binds selectively to GM1. Additionally, we assumed that the overabundance of GM1 among other glycans recognized by cholera toxin in the brain justifies its use as a GM1 marker (Schnaar et al., 2014). After rinsing, the nuclei were stained with DAPI diluted to a concentration of 1 μg/ml for 10 min at +4°C and rinsed again in PBS. The microscope, magnification, and image resolution were the same as those used in the single fluorescent staining.

2.7 | Immunohistochemical quantification and a newly developed Python script

All quantification analyses were performed by a researcher uninvolved in the experiments. The cell count of GFAP and Iba1 and the surface areas of APP-positive cells were analyzed in the CA1 and DG regions. The surface areas of AMPA-R-positive cells were analyzed in the CA1, CA2, and DG regions. All stainings were quantified with the Fiji software (Wayne Rasband, National Institutes of Health, USA). The total analyzed surface area in each hippocampal region was 0.01 mm^2. After adjusting the threshold according to the negative control, the integrated

density was measured. At least five biological replicates were used for microscopy. AMPA-R and APP images were analyzed with the integrated density value (IDV) plugin of the Fiji software (Schindelin et al., 2012). Fluorescent triple stainings were analyzed with a custom Python script. In the analysis of pixel intensities, a thresholding operation was used to reduce 16-bit images into binary ones. In this step, the pixel intensity value was replaced by a binary "1" or "0" if the molecule of interest was present or absent, respectively, at certain image coordinates. A threshold differentiating between pixel intensity values that should be treated as logical "1" or "0" was set for every sample and every imaging channel based on the control experiments. To calculate the colocalization between the channels, we applied logical AND operation for every pair of double or triple (GD1a/GM1/Np65) channel combinations. The resulting binary image represented the colocalized pixels, which were counted and used for further analysis as absolute values with respect to the total number of pixels that passed the thresholding. The triple stainings data were used to create pie charts illustrating the membrane disarrangement upon stress and aging. The pie charts included absolute pixel count of all channels. To illustrate the membrane composition and avoid the loss of pixel count when creating the pie chart, we applied the following formulas:

$$\mathrm{Ch1_{tot}} = \mathrm{Ch1_{nCL}} + (\mathrm{dCL_{1/2}} - \mathrm{tCL}) + (\mathrm{dCL_{1/3}} - \mathrm{tCL}) + \mathrm{tCL},$$

where Ch1 stands for Channel 1, *tot* is total pixel count, nCL are noncolocalized pixels, $\mathrm{dCL_{1/2}}$ or $\mathrm{dCL_{1/3}}$ are double colocalizations of Channel 1 and 2 or Channel 1 and 3, respectively, and tCL is triple colocalization. The same logic applies for $\mathrm{Ch2_{tot}}$ and $\mathrm{Ch3_{tot}}$. Therefore, to obtain the absolute pixel count for certain colocalization, which will be presented by a pie chart, the following formula applies:

$$\begin{aligned}\text{Absolute pixel count} &= \mathrm{Ch1_{tot}} + \mathrm{Ch2_{tot}} + \mathrm{Ch3_{tot}} \\ &= \mathrm{Ch1_{nCL}} + \mathrm{Ch2_{nCL}} + \mathrm{Ch3_{nCL}} + 2\times(\mathrm{dCL_{1/2}} - \mathrm{tCL}) + 2\times(\mathrm{dCL_{1/3}} - \mathrm{tCL}) + 2\times(\mathrm{dCL_{2/3}} - \mathrm{tCL}) + 3\times\mathrm{tCL}.\end{aligned}$$

The CA1 and DG hippocampal regions stained with Np65 and GM1 were 3D-reconstructed with confocal microscopy. Tissue reconstructions were described qualitatively. The colocalization of both markers in different z-sections was 3D-assembled by confocal microscopy at 40× magnification (oil immersion) using a Leica SP8 microscope and the matching LAS X Leica software.

2.8 | Statistical analysis

All statistical analyses were performed by a researcher uninvolved in the experiments. Statistical analysis of passive avoidance was performed in Python software with the Cox regression modeling and chi-square test in old females. Statistical analysis of immunostaining was performed with Statistica 12 software (TIBCO, Palo Alto, CA, USA). A p-value of <0.05 was considered significant. The two-way ANOVA was performed to determine the influence of stress, age, and their interaction on the analyzed parameters. Bonferroni correction was used for post hoc comparisons. The normality of data distribution was tested with the Shapiro–Wilk test.

3 | RESULTS

3.1 | Memory impairment

Memory impairment, tested by passive avoidance test, was present in 90% of stressed old females compared with 40% of the control group. Cox regression modeling revealed a greater hazard ratio for the effect of age. However, the effect did not reach significance, probably due to data uniformity among young animals (all young animals spent the maximum 180 s in the apparatus). Higher memory impairment in old stressed females was significant when compared to old control group of females ($\chi^2 = 5.22$, $df = 1$, $p = 0.022$) (Figure 2).

3.2 | Chronic stress dysregulates immune response in the hippocampus

Microglia dynamics in response to aging and chronic stress recovery in the CA1 and DG regions was evaluated by determining the Iba1-positive cell count and IDV (Figure 3). Young and old stressed females had a reduced microglial cell number in the hippocampal regions, but no significant difference was observed. IDV in the DG followed the cell count, but in the CA1 the opposite effect was observed—while cell number decreased, IDV in both animal groups increased upon stress (CA1, age: $F_{1,24} = 15.96$, $p = 0.001$ and DG, stress: $F_{1,24} = 12.52$, $p = 0.002$; interaction of stress and aging: $F_{1,24} = 16.25$, $p = 0.021$). We can speculate that in the CA1 region, increased IDV and decreased cell number represent the microglia activation upon stress.

Astroglial response to aging and stress was estimated by determining the GFAP-positive cell count (Figure 4). Both stressed animal groups had significantly increased astroglial cell number in the CA1 region ($F_{1,24} = 8.67$, $p = 0.007$). However, in the DG, astroglial cell number decreased in

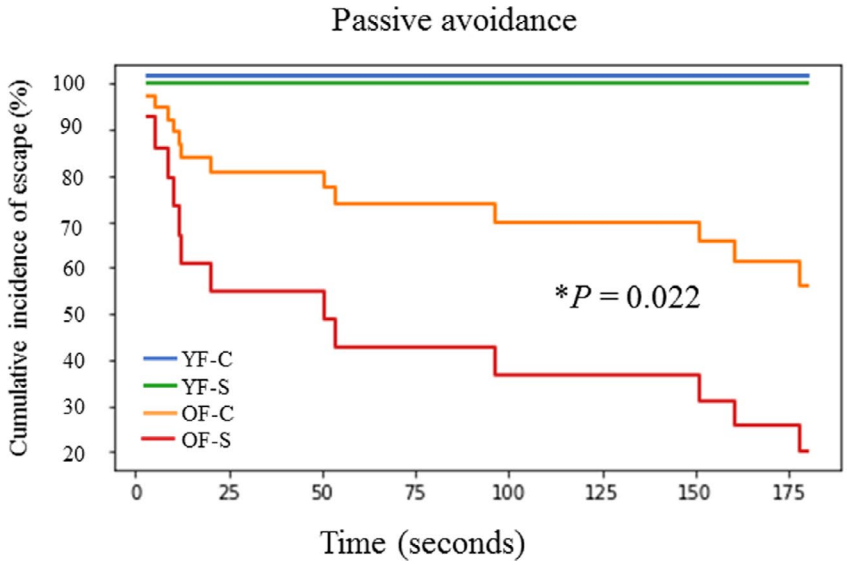

	Cox regression modeling		
	Hazard Ratio	[95% -CI]	*P*-value
Age	322388.28	0.000	0.920
Stress	2.78	0.839	0.094

FIGURE 2 Effect of chronic stress and aging on memory impairment in young and old female rats assessed with a passive avoidance test at the end of the study. The latency to enter the dark compartment 24 hr following the initial training (when foot-shock was applied) was recorded for 180 s. If the rats did not enter the dark compartment for 180 s, the successful acquisition of passive avoidance response was recorded. The results are shown as latencies (seconds) in a cumulative incidence plot. Statistical analysis was performed using a Cox regression modeling (table) and chi-square test for comparison of the two old groups. Statistical significance between control and stressed old females is marked with an asterisk. Abbreviations: CI, confidence interval; OF-C, control group of old females; OF-S, stressed group of old females; YF-C, control group of young females; YF-S, stressed group of young females

young stressed females and increased in old stressed females, with age and age–stress interaction reaching significance (age: $F_{1,24} = 7.99$, $p = 0.009$; interaction: $F_{1,24} = 11.26$, $p = 0.003$). The number of GFAP-positive cells significantly decreased in the old control group compared with the young control group (Bonferroni post hoc analysis $p < 0.001$). GFAP-positive cell count in the DG followed the trend of IDV (data not shown).

3.3 | Chronic stress conditions affect synaptic plasticity

AMPA-R expression in the CA1, CA2, and DG regions was assessed because of its involvement in long-term potentiation (Figure 5). Aging significantly affected AMPA-R expression in the CA2 region ($F_{1,19} = 5.034$, $p = 0.037$). Additionally, a post hoc between-group comparison revealed that age underlied AMPA-R decrease in the CA2 of old stressed females compared with young stressed females ($p = 0.006$). The interaction of aging and stress profoundly affected AMPA-R expression in both the CA2 and DG regions (CA2: $F_{1,19} = 5.083$, $p = 0.036$, DG: $F_{1,19} = 4.673$, $p = 0.044$). Stress significantly decreased AMPA-R expression in the DG region of old animals ($F_{1,19} = 5.464$, $p = 0.031$). Thus, AMPA-R expression was more profoundly reduced in the CA2 and DG than in the CA1 due to both aging and long-term consequences of stress and are reflected in memory test (Figure 5b).

3.4 | Chronic stress increases the expression of amyloid precursor protein

APP expression was analyzed by immunofluorescence in the CA1 and DG regions (Figure 6). APP expression in the CA1 increased in young stressed females, but was even higher in both groups of old females, with the main effects reaching significance (age, $F_{1,16} = 8.521$, $p = 0.01$; stress, $F_{1,16} = 89.925$, $p < 0.001$). In the DG, it was significantly affected by the interaction of stress and aging ($F_{1,16} = 5.056$, $p = 0.039$), with the increase observed only in old stressed females. Generally, the staining intensity for the DG region was lower compared with that for the CA1.

3.5 | Compromised neuroplasticity upon chronic stress recovery

We explored the colocalization of neuroplastin with GD1a and GM1 in the CA1 and DG regions. Pie charts representing the absolute pixel count for single, double, and triple combinations were used to illustrate the membrane disorganization as a result of stress and aging (Figures 7 and 8). In the CA1 region of the young female group, chronic

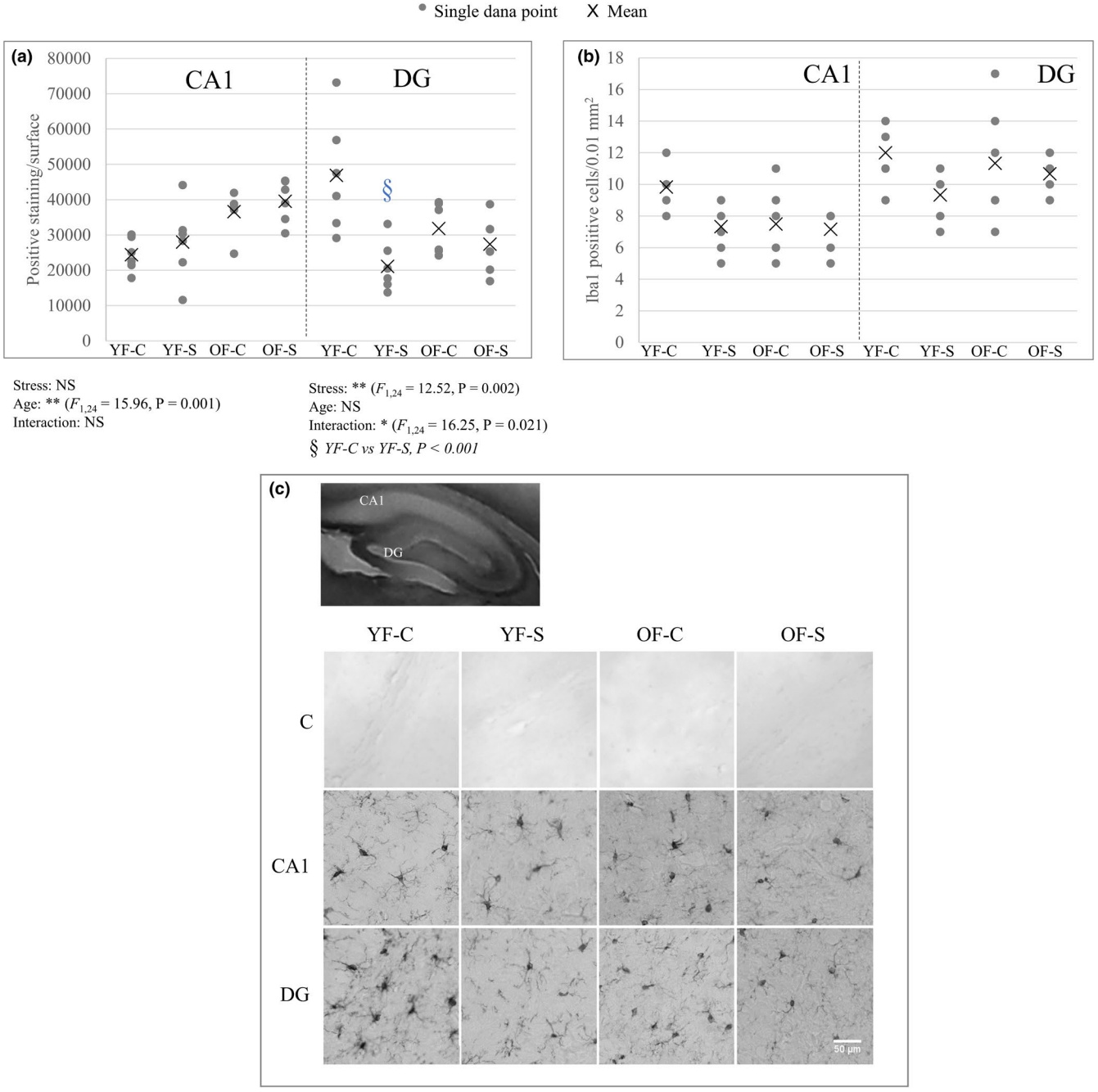

FIGURE 3 The quantitative and qualitative analysis of Iba1 positive cells in the CA1 and DG hippocampal regions in young and old female rats upon chronic stress. Iba1-positive staining (measured as integrated density value) is shown in (a). Microglia cell number decreased in both young and old stressed females in the CA1 and DG, but no statistical significance was reached (b). Image inserts are shown in (c). Significant main effects and their interaction are marked as follows: $*p < 0.05$, $***p < 0.001$. Significant difference between the groups is marked by a § symbol, and the exact *P*-value is indicated. Abbreviations: C, negative control reaction; CA1, *Cornu Ammonis* subfield 1; DG, dentate gyrus; Iba1, ionized calcium binding adaptor molecule 1; NS, nonsignificant; OF-C, control group of old females; OF-S, stressed group of old females; YF-C, control group of young females; YF-S, stressed group of young females

stress did not dramatically change the shares of the three membrane components or their colocalizations. However, in old stressed animals, the ratios of Np65 (main effect of age: $F_{1,25} = 94.052$, $p < 0.001$), GD1a (main effect of age: $F_{1,25} = 40.901$, $p < 0.001$, stress: $F_{1,25} = 38.439$, $p < 0.001$ and their interaction: $F_{1,25} = 39.328$, $p < 0.001$), and all double and triple staining combinations (main effect of stress: $F_{1,25} = 6.206$, $p = 0.02$) increased at the expense of GM1 (main effect of age: $F_{1,25} = 108.406$, $p < 0.001$ and stress: $F_{1,25} = 26.608$, $p < 0.001$) compared with old nonstressed females (Figure 7 and Table 1). Even though in young stressed females, free Np65 count (main effect

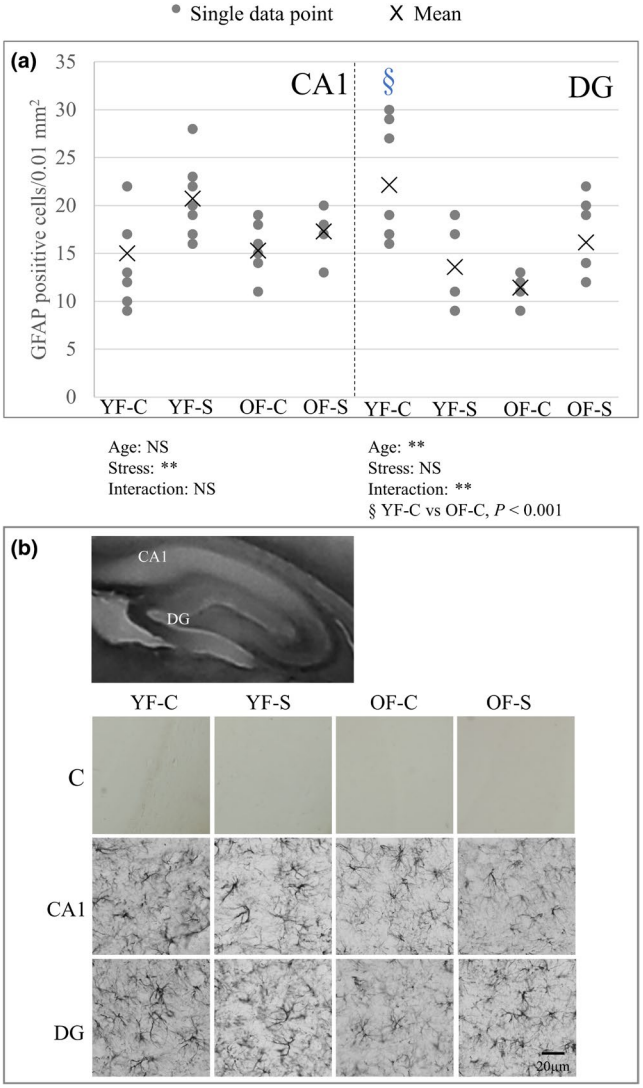

FIGURE 4 The quantitative analysis of glial fibrillary acidic protein (GFAP)-positive cells in the CA1 and DG hippocampal regions of young and old female rats upon chronic stress. Cell count for the astrocyte positive cells was analyzed in two hippocampal regions, CA1 and DG (a). Image inserts are shown in (b). Statistical analysis was performed using a two-way analysis of variance (ANOVA). Bonferroni correction was used for post hoc comparisons. Significant main effects and their interaction are marked as $*p < 0.05$, $***p < 0.001$. Significant difference between groups in the DG region is marked by a § symbol, and the exact *P*-value is indicated. Abbreviations: C, negative control reaction; CA1, *Cornu Ammonis* subfield 1; DG, dentate gyrus; GFA*P*, glial fibrillary acidic protein; NS, nonsignificant; OF-C, control group of old females; OF-S, stressed group of old females; YF-C, control group of young females; YF-S, stressed group of young females

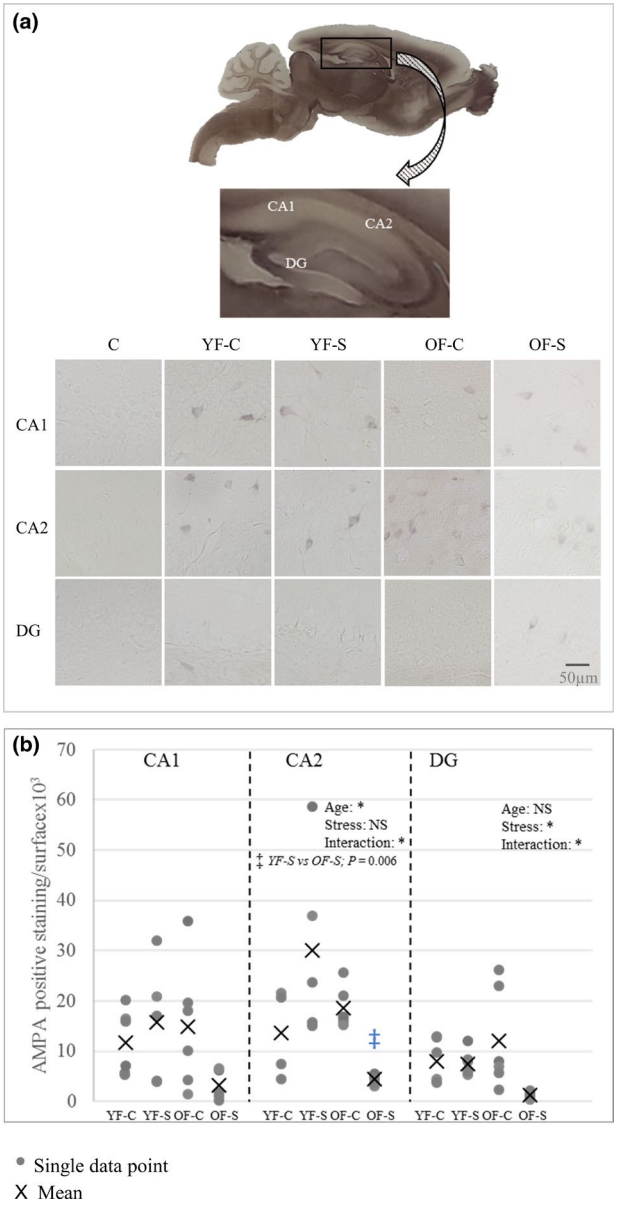

FIGURE 5 AMPA-R immunoreactivity in the hippocampal CA1, CA2 and DG regions in female rats in response to chronic stress and aging. (a) AMPA-R immunoreactivity was analyzed in three hippocampal regions by free-floating immunohistochemistry. (b) Statistical analysis was performed using a two-way analysis of variance (ANOVA). Bonferroni correction was used for post hoc comparisons. Significant effects of age or stress and their interaction are marked as $*p < 0.05$. A significant difference between groups in the CA2 region is marked by a ‡ symbol, and the exact *P*-value is indicated. Abbreviations: AMPA-R, AMPA-receptor; C, negative control reaction; CA1, *Cornu Ammonis* subfield 1; CA2, *Cornu Ammonis* subfield 2; DG, dentate gyrus; NS, nonsignificant; OF-C, control group of old females; OF-S, stressed group of old females; YF-C, control group of young females; YF-S, stressed group of young females

of age: $F_{1,22} = 163.987$, $p < 0.001$, stress: $F_{1,22} = 4.923$, $p = 0.037$ and their interaction: $F_{1,22} = 6.590$, $p = 0.018$) in the DG increased, its bound form was retained in the same environment. The share of Np65 colocalization with GM1 (main effect of age: $F_{1,22} = 5.864$, $p = 0.024$ and interaction of age with stress: $F_{1,22} = 12.712$, $p = 0.002$), GD1a (main effect of stress: $F_{1,22} = 5.883$, $p = 0.024$ and interaction of age with stress: $F_{1,22} = 37.591$, $p < 0.001$)

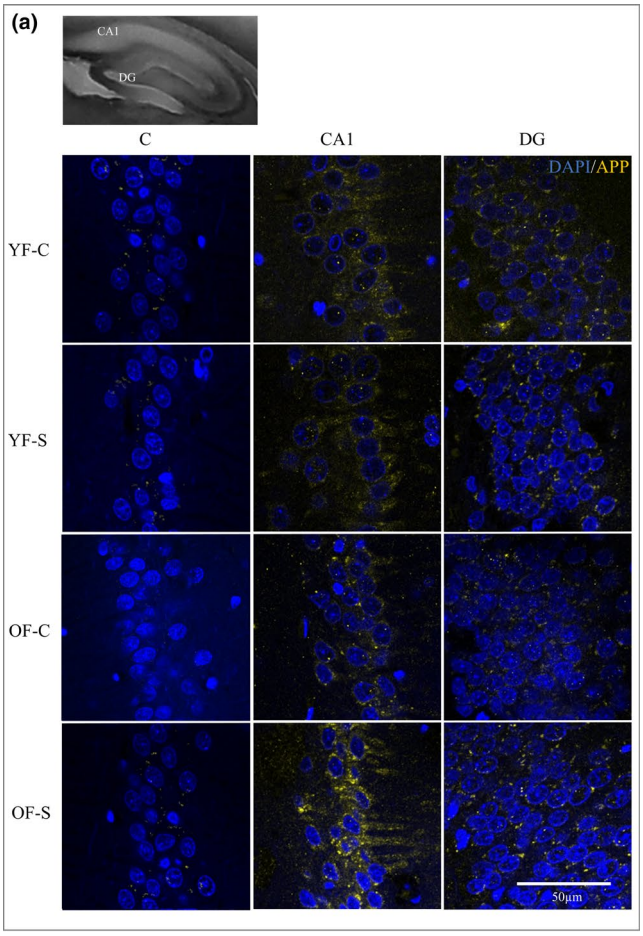

FIGURE 6 The quantitative analysis of APP expression in the CA1 and DG hippocampal regions of young and old stressed female rats. Image inserts are shown in (a). Immunofluorescent staining was analyzed using integrated density values for APP in the CA1 (B, on the left) and DG (b, on the right). Statistical analysis was performed using a two-way analysis of variance (ANOVA). Bonferroni correction was used for post hoc comparisons. Significant effects of age or stress and their interaction are marked as $*p < 0.05$, $***p < 0.001$. Abbreviations: AP*P*, amyloid precursor protein; CA1, *Cornu Ammonis* subfield 1; DG, dentate gyrus; NS, nonsignificant; OF-C, control group of old females; OF-S, stressed group of old females; YF-C, control group of young females; YF-S, stressed group of young females

as well as in triple colocalization remained similar (main effect of age: $F_{1,22} = 55.026$, $p < 0.001$ and interaction of age with stress: $F_{1,22} = 20.542$, $p < 0.001$). In old control females, the share of colocalized Np65 was different than in young animals, with a significant reduction of free neuroplastin (Figure 8 and Table 2). In response to stress and aging, GM1 increased, while GD1a and neuroplastin decreased, and colocalizations remained at a similar level.

IDVs were analyzed as a measure of molecules dispersion for GD1a, Np65 and GM1 in the CA1 and DG (Figure S1).

3.6 | Tissue reconstruction

Three-dimensional tissue reconstruction showed a decrease in Np65 staining in the CA1 region in young and old stressed animals, while GM1 remained unchanged (Figure 9a). In the DG region of young control animals, Np65 intensity of staining and the colocalization of Np65 and GM1 were more obvious in old stressed females, with an increased scattered pattern (Figure 9b).

4 | DISCUSSION

In this study, aging and stress inducted a memory decline in female rats despite a recovery period after stress exposure. Stress caused GM1 and GD1a ganglioside disorganization, a phenomenon affecting the trafficking of molecules associated with synaptic plasticity, such as APP, AMPA-R, and neuroplastin. Our results showed a GM1 decrease and GD1a increased in old stressed females. APP expression increased in both analyzed regions followed by astrocyte number increase, while neuroplastin increased only in the DG. AMPA-R decreased in the CA1, CA2, and DG regions in old stressed females. These findings complement the growing literature demonstrating a deterioration of cognitive performance in stressful conditions (Conrad et al., 1999, 2017; Luine et al., 1994; Woo et al., 2018).

Chronic stress strongly affected neuroinflammation, neuroplasticity, amyloidogenesis, and neurodegeneration in older animals. Microglia activation has been reported in GM1 gangliosidosis mice, supporting the idea that alterations in glycosphingolipid content cause central nervous neuroinflammation (Belarbi et al., 2020; Jeyakumar et al., 2003). We observed significant changes in response to stress and aging in astrocyte cell count but not in microglia count. Nevertheless, a trend of microglia count reduction in stressed animals was clearly visible, which could support the role of stress in the modulation of microglial structure and function (Walker et al., 2013). We can hypothesize that in the CA1

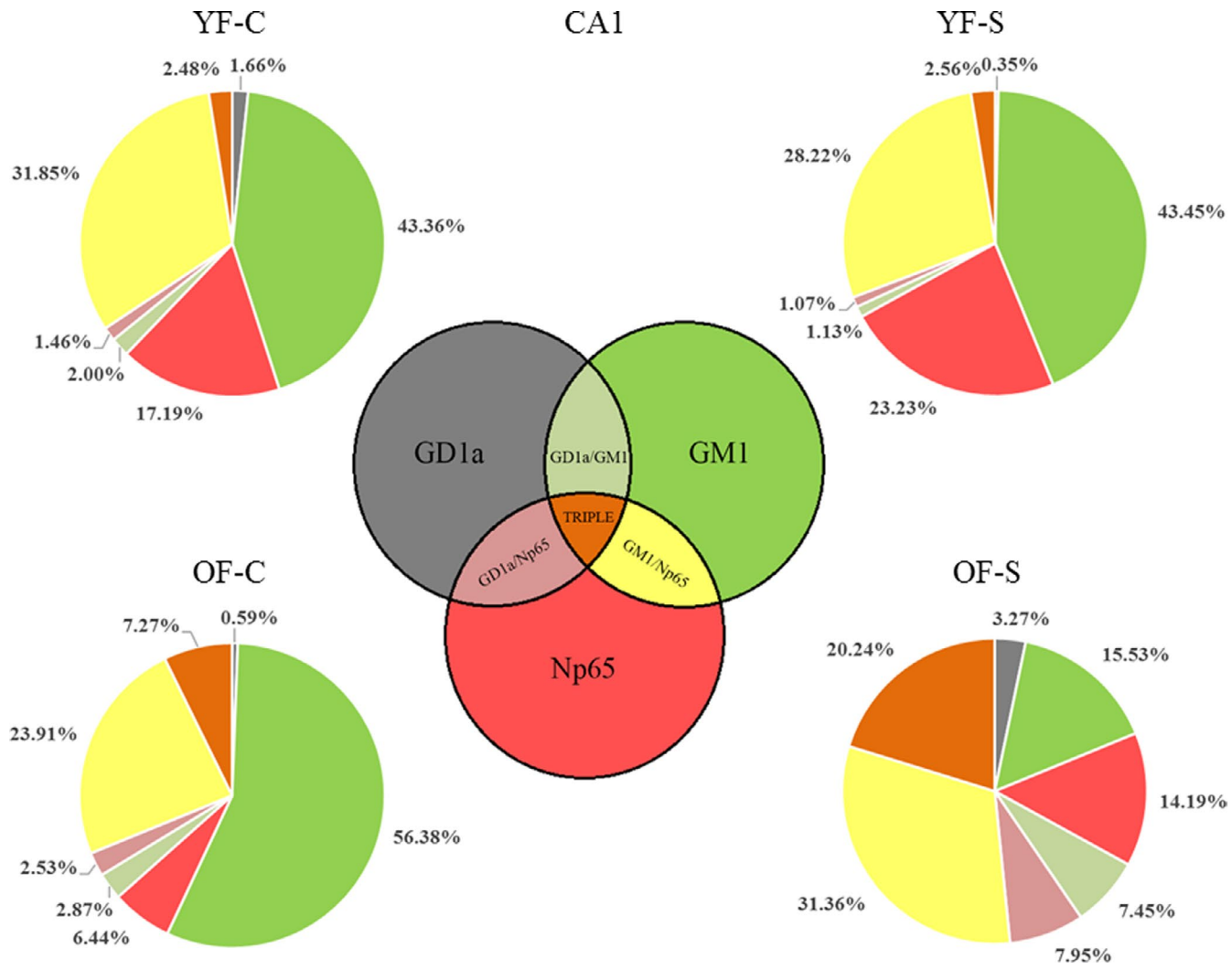

FIGURE 7 Age-specific changes in GM1, GD1a, and neuroplastin expression upon chronic stress in the CA1 hippocampal region. Immunofluorescent staining was analyzed using the shares of single molecules: GD1a, GM1 and Np65; double colocalizations: GD1a/Np65, GM1/Np65, GD1a/GM1; and triple colocalization in absolute pixel counts for all four animal groups. The average ratio of pixel count is shown for each single or combination profile. The Venn diagram defines the expression of combination profiles. Statistical analysis was performed using a two-way analysis of variance (ANOVA) and is shown in Table 1. Abbreviations: CA1, *Cornu Ammonis* subfield 1; GD1a, ganglioside GD1a; GM1, ganglioside GM1 visualized by cholera toxin beta subunit; NS, nonsignificant; Np65, neuroplastin; OF-C, control group of old females; OF-S, stressed group of old females; YF-C, control group of young females; YF-S, stressed group of young females

region specifically, increased IDV and decreased cell number imply the microglia activation upon stress. In contrast, increased astrocyte number in both stressed groups in CA1 and in old females in DG suggested a glial inflammatory effect. According to the literature, reactive astrocytes can indicate glutamate homeostasis dysregulation (Palpagama et al., 2019). Moreover, this finding is in accordance with our results concerning AMPA-R–AMPA-R expression significantly decreased in old stressed animals in the CA2 and DG regions, while the number of astrocytes significantly increased in the DG region. Additionally, the expression pattern of astrocytes was followed by APP expression. The relationship between astrocyte number and APP expression observed in our study might imply an interplay of astrocytes and APP-expressing cells of the brain. Previously, astrocytes were found in a vicinity of amyloid plaques (Rossi & Volterra, 2009), suggesting their involvement in APP processing and consecutively amyloid-β formation and triggering of neurodegenerative processes.

Neuroplastin interacts with the HPA axis, directly influencing stress response and cognition (Beesley et al., 2014; Bhattacharya et al., 2017). It has been hypothesized than neuroplastin depends on the lipid environment (Ilic et al., 2019), so we analyzed it together with GM1 and GD1a gangliosides. The two gangliosides were studied together because GD1a acts as a reservoir of GM1–GM1 can be synthesized from GD1a apart from its classical synthesis (Miyagi & Yamaguchi, 2012; Sonnino

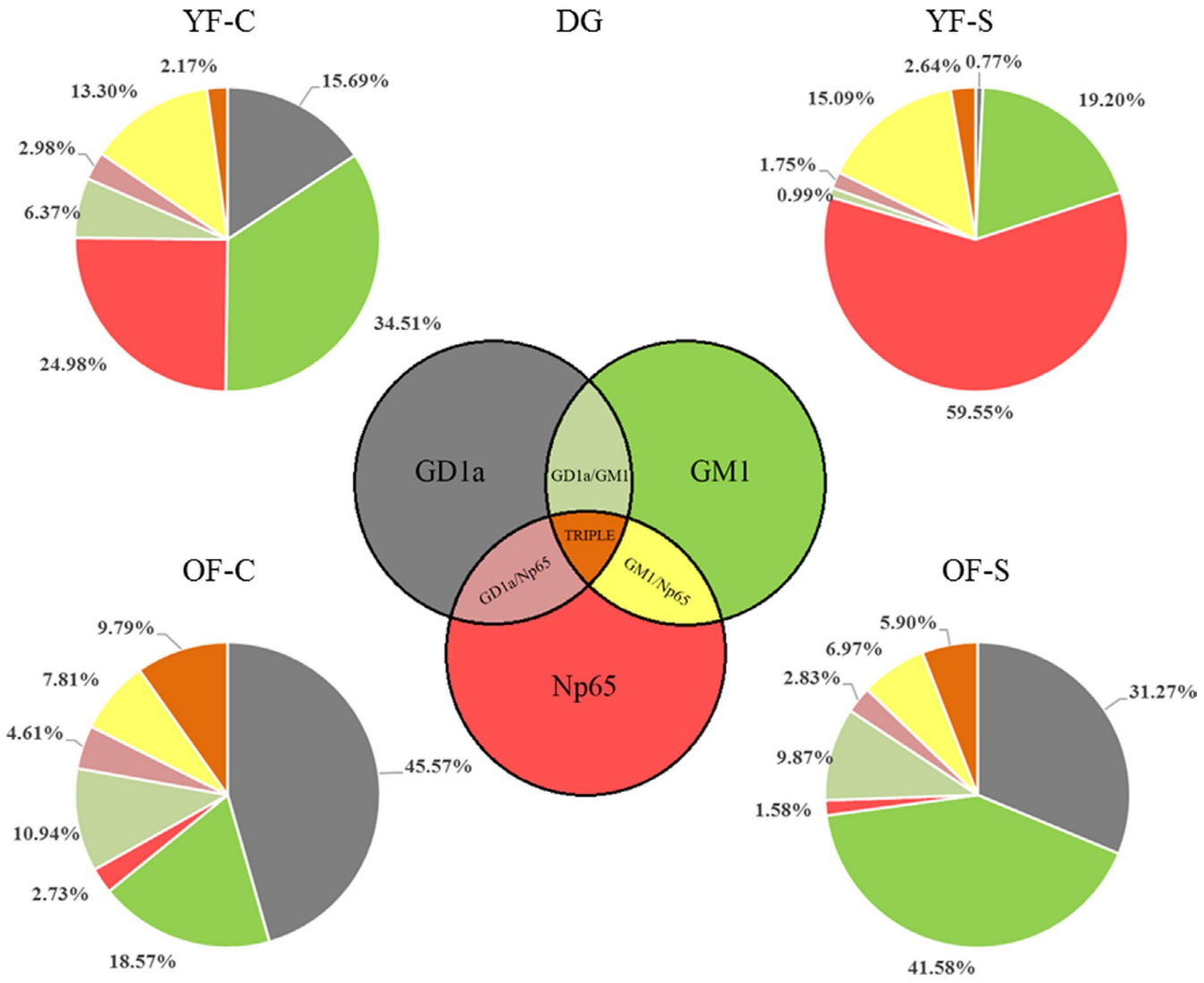

FIGURE 8 Age-specific changes in GM1, GD1a, and neuroplastin expression upon chronic stress in the DG hippocampal region. Immunofluorescent staining was analyzed using the shares of single molecules: GD1a, GM1, and Np65; double colocalizations: GD1a/Np65, GM1/Np65, GD1a/GM1; and triple colocalization in absolute pixel counts for all four animal groups. The average ratio of pixel count is shown for each single or combination profile. The Venn diagram defines the expression of combination profiles. Statistical analysis was performed using a two-way analysis of variance (ANOVA) and is shown in Table 2. Abbreviations: CA1, *Cornu Ammonis* subfield 1; GD1a, ganglioside GD1a; GM1, ganglioside GM1 visualized by cholera toxin beta subunit; NS, nonsignificant; Np65, neuroplastin; OF-C, control group of old females; OF-S, stressed group of old females; YF-C, control group of young females; YF-S, stressed group of young females

et al., 2011) and it was previously found to be implicated in neurodegenerative processes (Chiricozzi et al., 2020; Kolyovska, 2016). GD1a concentration in the frontal brain decreases with aging (Svennerholm et al., 1989), and a similar decrease was observed in AD patients, especially in the hippocampus (Mesa-Herrera et al., 2019; Svennerholm, 1994).

The shares of all three markers (GM1, Np65, and GD1a) and their combinations (Figures 7 and 8) provided information of each epitope and its interactions in the total number of molecules observed at a given location. We calculated these shares to analyze the changes in the membrane architecture. When the total pixel number was divided in single, double, and triple staining, the shares of neuroplastin contributions (i.e. GM1/Np65, GD1/Np65) in young stressed animals were not changed, and neuroplastin environment in the CA1 remained constant. In old females, however, the shares of free GM1 and free neuroplastin changed—GM1 decreased and neuroplastin increased. If aging was observed without stress—a neuroplastin decrease was obvious, while its double colocalizations remained invariable and triple colocalization increased. Altogether, stress in young animals and stress-free aging in the CA1 region can be figuratively described as playing the same game with fewer players on the field. When aged animals are exposed to stress, there are too few players on the field to deal with additional challenges:

TABLE 1 Statistical significance of the GD1a/GM1/Np65 staining in the CA1 region

Molecule/overlap combinations	Statistical significance of the main effects or their interactions in CA1 region			Post hoc (Bonferroni)
	Age	Stress	Interaction	
GD1a	$F_{1,25} = 40.901$, $p < 0.001$	$F_{1,25} = 38.439$, $p < 0.001$	$F_{1,25} = 39.328$, $p < 0.001$	*YF-C* versus *YF-S*, $p < 0.001$
GM1	$F_{1,25} = 108.406$, $p < 0.001$	$F_{1,25} = 26.608$, $p < 0.001$	NS	-
Np65	$F_{1,25} = 94.052$, $p < 0.001$	NS	NS	-
GD1a/GM1	$F_{1,25} = 20.028$, $p < 0.001$	$F_{1,25} = 22.606$, $p < 0.001$	$F_{1,25} = 5.917$, $p = 0.022$	*YF-C* versus *YF-S*, $p < 0.001$
GD1a/Np65	$F_{1,25} = 13.411$, $p = 0.001$	$F_{1,25} = 12.517$, $p = 0.002$	NS	-
Np65/GM1	$F_{1,25} = 122.564$, $p < 0.001$	$F_{1,25} = 29.788$, $p < 0.001$	NS	-
GD1a/GM1/Np65	NS	$F_{1,25} = 6.206$, $p = 0.02$	NS	-

Note: Statistical analysis was performed using a two-way ANOVA. Bonferroni correction was used for post hoc comparisons. Significant effects of stress or age and their interaction are marked as exact *p*-values.

Abbreviations: ANOVA, analysis of variance; CA1, *Cornu Ammonis* subfield 1; GD1a, ganglioside; GM1, ganglioside GM1 visualized by cholera toxin beta subunit; Np65, neuroplastin; NS, nonsignificant; OF-C, control group of old females; OF-S, stressed group of old females; YF-C, control group of young females; YF-S, stressed group of young females.

TABLE 2 Statistical significance of the GD1a/GM1/Np65 staining in the DG region

Molecule/overlap combinations	Statistical significance of the main effects or their interactions in DG region			Post hoc (Bonferroni)
	Age	Stress	Interaction	
GD1a	$F_{1,22} = 20.625$, $p < 0.001$	NS	$F_{1,22} = 21.495$, $p < 0.001$	*YF-S* versus *OF-S*, $p < 0.001$
GM1	NS	NS	$F_{1,22} = 32.177$, $p = 0.000$	-
Np65	$F_{1,22} = 163.987$, $p < 0.001$	$F_{1,22} = 4.923$, $p = 0.037$	$F_{1,22} = 6.590$, $p = 0.018$	*YF-C* versus *YF-S*, $p = 0.002$; *YF-S* versus *OF-S*, $p < 0.001$
GD1a/GM1	$F_{1,22} = 7.173$, $p = 0.014$	NS	$F_{1,22} = 24.994$, $p < 0.001$	*YF-S* versus *OF-S*, $p < 0.001$
GD1a/Np65	NS	$F_{1,22} = 5.883$, $p = 0.024$	$F_{1,22} = 37.591$, $p < 0.001$	*YF-C* versus *YF-S*, $p < 0.001$; *OF-C* versus *OF-S*, $p = 0.019$
Np65/GM1	$F_{1,22} = 5.864$, $p = 0.024$	NS	$F_{1,22} = 12.712$, $p = 0.002$	-
GD1a/GM1/Np65	$F_{1,22} = 55.026$, $p < 0.001$	NS	$F_{1,22} = 20.542$, $p < 0.001$	*YF-S* versus *OF-S*, $p < 0.001$

Note: Statistical analysis was performed using a two-way ANOVA. Bonferroni correction was used for post hoc comparisons. Significant effects of stress or age and their interaction are marked as exact *p*-values.

Abbreviations: ANOVA, analysis of variance; DG, dentate gyrus; GD1a, ganglioside; GM1, ganglioside GM1 visualized by cholera toxin beta subunit; Np65, neuroplastin, OF-C, control group of old females; NS, nonsignificant; OF-S, stressed group of old females; YF-C, control group of young females; YF-S, stressed group of young females.

GM1 is consumed in the interaction with neuroplastin and GD1a, while GD1a enters the field (increased expression) as a back-up for GM1. These findings are summarized in Figure 10, where we propose a potential model of neuroplastin interaction with the two ganglioside species in the membrane lipid microenvironments. Each specific environment might influence neuroplastin functionality, and specific combinations could underlie synaptic dysfunction. The strongest cognitive decline was observed in old stressed females, who had a GD1a-rich environment in their CA1 and DG.

The CA1 and DG perform different functions (Barth et al., 2018), which were reflected in our analysis of membrane architecture. In the DG of young stressed females, free neuroplastin share increased and the GM1 and GD1a count decreased. These changes consumed the available GD1a molecules alone or in interactions, extensively changing the

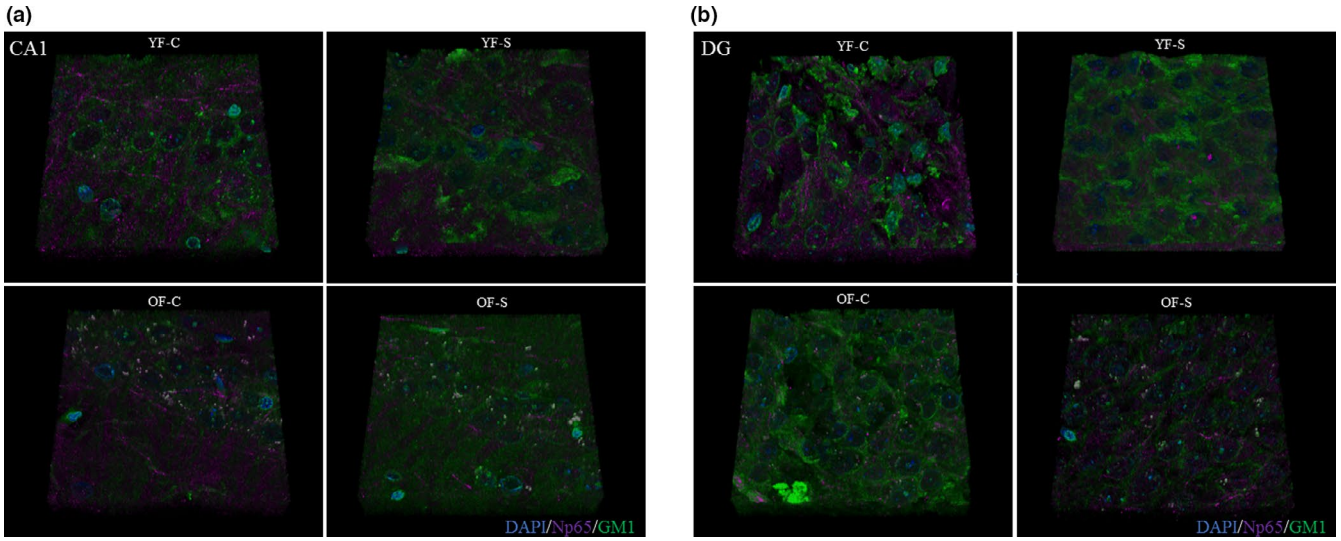

FIGURE 9 Immunofluorescent 3D reconstruction of the hippocampal CA1 (a) and DG (b) regions stained with Np65 and GM1 in young and old stressed female rats. The CA1 and DG hippocampal regions were reconstructed using confocal microscopy. Sagittal sections from the triple staining (Np65/GD1a/GM1) were used. For the reconstruction, two channels were used because of the confocal microscope limitations, so Np65/GM1 colocalization was analyzed. The colocalization of both markers in different z-sections was 3D-assembled by confocal microscopy at 40× (oil immersion). Np65 is stained magenta, GM1 is stained green, while nuclei are blue. Abbreviations: GM1, ganglioside GM1 visualized by cholera toxin beta subunit; Np65, neuroplastin; OF-C, control group of old females; OF-S, stressed group of old females; YF-C, control group of young females; YF-S, stressed group of young females

membrane architecture. In aged animals, free neuroplastin almost completely disappeared from the DG membranes, while elevated GD1a expression compensated for GM1 decrease. When we added stress to aging, the main effect was free GD1a increase compared with young animals, which probably means that neuroplastin in the DG does not use the available GD1a for interaction.

An additional stress mechanism in reproductive senescence was revealed by IDV analysis. Young stressed females experienced a decreased expression of both gangliosides, while old stressed females experienced a decreased GM1 expression and an increased GD1a expression in both hippocampal regions. Neuroplastin in the CA1 decreased upon stress independently from aging. However, in the DG of old stressed females, neuroplastin expression increased.

IDV can be considered as the membrane epitope scattering measure (Pavel et al., 2020). Based on IDV analysis, we propose that aging generally decreases the diameter of individual microdomains and seriously compromises their function, that is, in synaptogenesis.

Overall, the pie charts revealed the players in the CA1 and DG membrane architecture and their changes in response to stress and aging, while IDV supported the idea that in such conditions neuroplastin changes, as well as its environment.

A 3D tissue reconstruction presented the complexity of the CA1 and DG regions. Although the reconstructed images pointed to qualitative peculiarities of both regions, the method's limitations, such as rapid photobleaching and bleed-through between channels, prevented us from performing anything more than qualitative analysis. Due to the technical limitations, only two molecules, neuroplastin and GM1, were chosen for reconstruction. The expressions of both molecules decreased in response to stress and aging, except in the DG of old stressed females, where neuroplastin increased but became more scattered. This effect might be attributed to the association of neuroplastin with GD1a but not with GM1.

Future studies might further elucidate these processes by biochemical isolation of lipid rafts. However, hippocampal regions with different functions, such as the CA1 and DG, would be challenging to separate. In addition, all lipid rafts isolation protocols involve the use of detergents. In this study, we intentionally did not use detergents as they were shown in our previous study to lead to glycolipid transfer into the adjacent membranes even in fixed tissue (Heffer-Lauc et al., 2005). As our study's focus was the glycolipid environment of neuroplastin as a basis for memory deficit in older females exposed to stress, we focused on a detailed analysis of immunohistochemical results. To the best of our knowledge, this is the only study providing a detailed in situ analysis of glycosphingolipids as a response to aging and stress.

The interpretation of memory impairment process could be facilitated by performing additional behavioral tests or by performing the passive avoidance test at the beginning and end of the study. Additional behavioral data would have allowed us to better understand memory impairment fluctuation during the study. However, as the passive avoidance test strongly activates the amygdala, hippocampus, and entorhinal cortex (Izquierdo et al., 1997), it was performed only once.

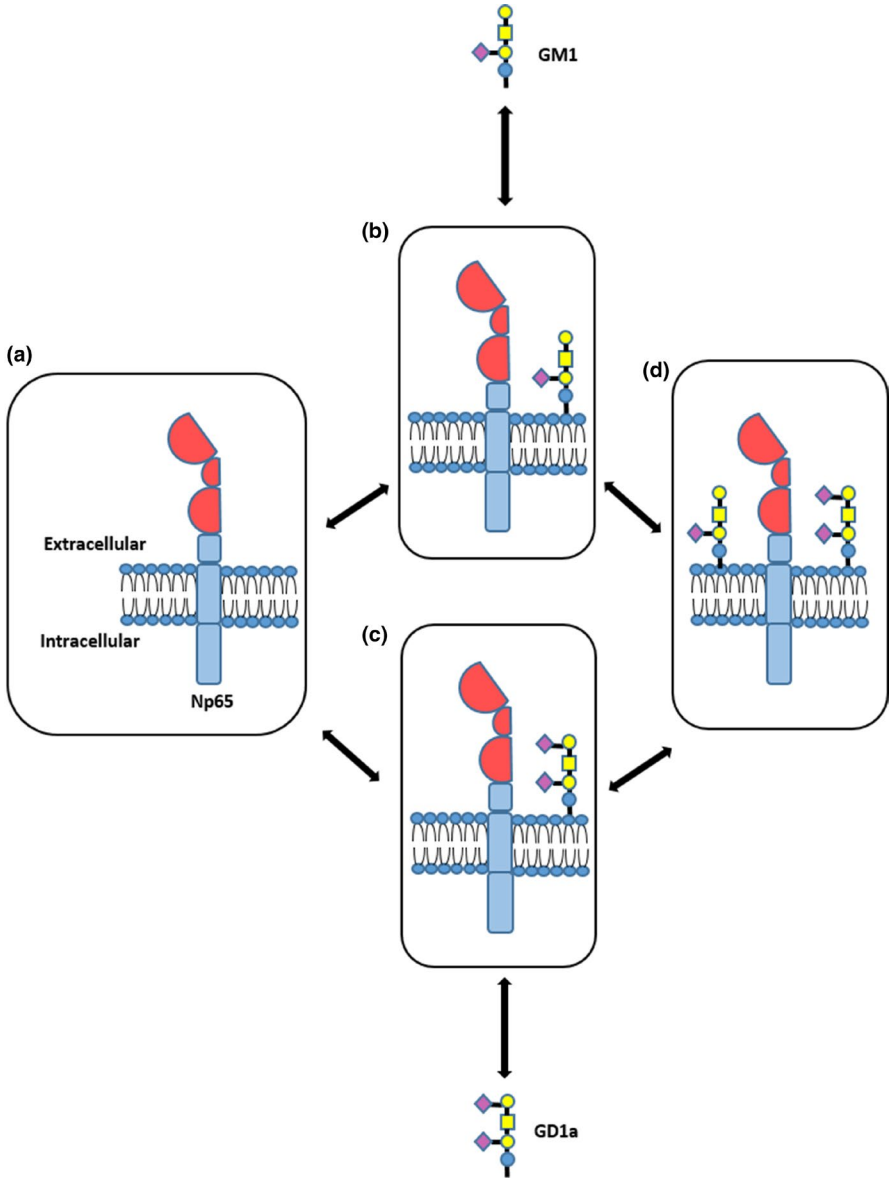

FIGURE 10 Possible ganglioside membrane environments of neuroplastin in the CA1 and DG hippocampal regions based on GD1a/GM1/Np65 analysis. Four possible membrane environments were postulated: (a) Neuroplastin can stand alone. It could be localized in an environment rich in GM1 (b), GD1a (c), or both gangliosides (d). Abbreviations: GD1a, ganglioside GD1a; GM1, ganglioside GM1; Np65, neuroplastin

Nonstressful tests, such as the object location memory test, that would be required to differentiate the effects of aging and stress on memory changes compared with the changes in the fear/stress response to the shock during the passive avoidance memory test were not available.

Memory is known to be affected by the hormonal status (Ali et al., 2018), but we did not determine the estrous stage for several reasons. If we had paired the animals according to the estrous stage, the number of animals per group would not have reached the expected sample size. Even if the animals entered the study with the same hormonal status, we expected desynchronization due to dysregulation of the gonadal axis by chronic stress (An et al., 2020; Lovick, 2012), especially considering the long study duration. Additional desynchronization was expected due to the (pre)menopausal age of the older animal group (Cruz et al., 2017).

Overall, this study suggests that chronic stress response did not affect the cognition of young female rats, even though some of the investigated molecules were expressed differently. However, old females exhibited diminished memory in response to both stress and aging. Cognitive dysfunction in reproductively senescent females might be underlied by expressional changes in the lipid environment of APP, neuroplastin, AMPA-R, glial cell number, as well as structural changes of the membrane lipids. The postulation of four possible neuroplastin environments pointed to GD1a enrichment in old stressed female rats, as well as its high dispersion in both hippocampal areas. The specific lipid environment might influence neuroplastin functionality, underlying synaptic dysfunction and amyloidogenesis triggered by the combination of aging and chronic stress.

In conclusion, our newly developed Python method proved to be a useful tool for the analysis of membrane

microenvironments in situ, which makes it suitable for use in similar studies.

ACKNOWLEDGEMENTS

This study was supported by Cedars-Sinai Medical Center's International Research and Innovation in Medicine Program and the Association for Regional Cooperation in the Fields of Health, Science and Technology (RECOOP HST Association). The RECOOP-Cedars Research Centers (CRRCs) received the Bohdan Malaniak CSMC - RECOOP Young Scientists Research Grants: RECOOP # 001 BMYS RG Balog, "Impact of acute and chronic stress on cardiovascular diseases" and RECOOP # 019 BMYS RG Krajnik, "Lipid rafts of an Alzheimer's disease cellular model visualized by super-resolution fluorescence microscopy"; Croatian Science Foundation through research grants IP-2014-09-2324; grant SAF2017-85554-R from Spanish Ministry of Science and Innovation; European Union through the European Regional Development Fund, Operational Programme Competitiveness, and Cohesion, grant agreement no. KK.01.1.1.01.0007, CoRE–Neuro and through ERASMUS KA1 grants. This work was also supported by the Ministry of Human Capacities (Hungary grant 20391-3/2018/FEKUSTRAT).

CONFLICTS OF INTEREST

The authors have no conflict of interest to declare.

AUTHOR CONTRIBUTIONS

MB, RG, SGV, and MH: conceptualized the study and designed methodology; MB, VI, SB, AB, ACA, DPP, and KFS: carried out investigation and acquired the formal analysis; BK, IL, RG, AB, SGV, RM, and MH: analyzed or interpreted the data, reviewed, and edited the manuscript; MB: writing–original draft. All authors critically revised the manuscript for important intellectual content; all authors gave final approval of the version to be submitted; all authors agree to be held accountable for all aspects of the work.

PEER REVIEW

The peer review history for this article is available at https://publons.com/publon/10.1111/ejn.15256.

DATA AVAILABILITY STATEMENT

All the article's supporting data and materials can be accessed upon request from the corresponding author.

ORCID

Marta Balog https://orcid.org/0000-0002-7842-4781

REFERENCES

Aisen, P. S., Davis, K. L., Berg, J. D., Schafer, K., Campbell, K., Thomas, R. G., Weiner, M. F., Farlow, M. R., Sano, M., Grundman, M., & Thal, L. J. (2000). A randomized controlled trial of prednisone in Alzheimer's disease. *Neurology*, *54*(3), 588. https://doi.org/10.1212/wnl.54.3.588

Ali, S. A., Begum, T., & Reza, F. (2018). Hormonal influences on cognitive function. *The Malaysian Journal of Medical Sciences*, *25*(4), 31–41. https://doi.org/10.21315/mjms2018.25.4.3

An, G. H., Chen, X. W., Li, C., Zhang, L. I., Wei, M. F., Chen, J. J., Ma, Q., Yang, D. F., & Wang, J. (2020). Pathophysiological changes in female rats with estrous cycle disorder induced by long-term heat stress. *BioMed Research International*, *2020*, 4701563. https://doi.org/10.1155/2020/4701563

Balog, M., Miljanović, M., Blažetić, S., Labak, I., Ivić, V., Viljetić, B., & Heffer, M. (2015). Sex-specific chronic stress response at the level of adrenal gland modified sexual hormone and leptin receptors. *Croatian Medical Journal*, *56*(2), 104–113. https://doi.org/10.3325/cmj.2015.56.104

Barth, A. M., Domonkos, A., Fernandez-Ruiz, A., Freund, T. F., & Varga, V. (2018). Hippocampal network dynamics during rearing episodes. *Cell Reports*, *23*(6), 1706–1715. https://doi.org/10.1016/j.celrep.2018.04.021

Beesley, P. W., Herrera-Molina, R., Smalla, K.-H., & Seidenbecher, C. (2014). The Neuroplastin adhesion molecules: Key regulators of neuronal plasticity and synaptic function. *Journal of Neurochemistry*, *131*(3), 268–283. https://doi.org/10.1111/jnc.12816

Belarbi, K., Cuvelier, E., Bonte, M.-A., Desplanque, M., Gressier, B., Devos, D., & Chartier-Harlin, M.-C. (2020). Glycosphingolipids and neuroinflammation in Parkinson's disease. *Molecular Neurodegeneration*, *15*(1), 59. https://doi.org/10.1186/s13024-020-00408-1

Bhattacharya, S., Herrera-Molina, R., Sabanov, V., Ahmed, T., Iscru, E., Stöber, F., Richter, K., Fischer, K.-D., Angenstein, F., Goldschmidt, J., Beesley, P. W., Balschun, D., Smalla, K.-H., Gundelfinger, E. D., & Montag, D. (2017). Genetically induced retrograde amnesia of associative memories after neuroplastin ablation. *Biological Psychiatry*, *81*(2), 124–135. https://doi.org/10.1016/j.biopsych.2016.03.2107

Blennow, K., Davidsson, P., Wallin, A., Fredman, P., Gottfries, C.-G., Karlsson, I., Mansson, J.-E., & Svennerholm, L. (1991). Gangliosides in cerebrospinal fluid in 'probable Alzheimer's disease'. *Archives of Neurology*, *48*(10), 1032–1035. https://doi.org/10.1001/archneur.1991.00530220048018

Bussian, T. J., Aziz, A., Meyer, C. F., Swenson, B. L., van Deursen, J. M., & Baker, D. J. (2018). Clearance of senescent glial cells prevents tau-dependent pathology and cognitive decline. *Nature*, *562*(7728), 578–582. https://doi.org/10.1038/s41586-018-0543-y

Carter, T. L., Rissman, R. A., Mishizen-Eberz, A. J., Wolfe, B. B., Hamilton, R. L., Gandy, S., & Armstrong, D. M. (2004). Differential preservation of AMPA receptor subunits in the hippocampi of Alzheimer's disease patients according to Braak stage. *Experimental Neurology*, *187*(2), 299–309. https://doi.org/10.1016/j.expneurol.2003.12.010

Chang, E. H., Savage, M. J., Flood, D. G., Thomas, J. M., Levy, R. B., Mahadomrongkul, V., Shirao, T., Aoki, C., & Huerta, P. T. (2006). AMPA receptor downscaling at the onset of Alzheimer's disease pathology in double knockin mice. *Proceedings of the National Academy of Sciences of the United States of America*, *103*(9), 3410–3415. https://doi.org/10.1073/pnas.0507313103

Chiricozzi, E., Lunghi, G., Di Biase, E., Fazzari, M., Sonnino, S., & Mauri, L. (2020). GM1 ganglioside is a key factor in maintaining the mammalian neuronal functions avoiding neurodegeneration.

International Journal of Molecular Sciences, *21*(3), 868. https://doi.org/10.3390/ijms21030868

Conrad, C. D., LeDoux, J. E., Magariños, A. M., & McEwen, B. S. (1999). Repeated restraint stress facilitates fear conditioning independently of causing hippocampal CA3 dendritic atrophy. *Behavioral Neuroscience*, *113*(5), 902–913. https://doi.org/10.1037//0735-7044.113.5.902

Conrad, C. D., Ortiz, J. B., & Judd, J. M. (2017). Chronic stress and hippocampal dendritic complexity: Methodological and functional considerations. *Physiology & Behavior*, *178*, 66–81. https://doi.org/10.1016/j.physbeh.2016.11.017

Cruz, G., Fernandois, D., & Paredes, A. H. (2017). Ovarian function and reproductive senescence in the rat: Role of ovarian sympathetic innervation. *Reproduction*, *153*(2), R59–R68. https://doi.org/10.1530/rep-16-0117

Díaz, M., Fabelo, N., Ferrer, I., & Marín, R. (2018). "Lipid raft aging" in the human frontal cortex during nonpathological aging: Gender influences and potential implications in Alzheimer's disease. *Neurobiology of Aging*, *67*, 42–52. https://doi.org/10.1016/j.neurobiolaging.2018.02.022

Dumas, J. A., Albert, K. M., Naylor, M. R., Sites, C. K., Benkelfat, C., & Newhouse, P. A. (2012). The effects of age and estrogen on stress responsivity in older women. *The American Journal of Geriatric Psychiatry*, *20*(9), 734–743. https://doi.org/10.1097/JGP.0b013e31825c0a14

Falconi, A. M., Gold, E. B., & Janssen, I. (2016). The longitudinal relation of stress during the menopausal transition to fibrinogen concentrations: Results from the Study of Women's Health Across the Nation. *Menopause*, *23*(5), 518–527. https://doi.org/10.1097/GME.0000000000000579

Heffer-Lauc, M., Lauc, G., Nimrichter, L., Fromholt, S. E., & Schnaar, R. L. (2005). Membrane redistribution of gangliosides and glycosylphosphatidylinositol-anchored proteins in brain tissue sections under conditions of lipid raft isolation. *Biochimica Et Biophysica Acta*, *1686*(3), 200–208. https://doi.org/10.1016/j.bbalip.2004.10.002

Hou, Q., Huang, Y., Amato, S., Snyder, S. H., Huganir, R. L., & Man, H. Y. (2008). Regulation of AMPA receptor localization in lipid rafts. *Molecular and Cellular Neurosciences*, *38*(2), 213–223. https://doi.org/10.1016/j.mcn.2008.02.010

Hung, C. W., Chen, Y. C., Hsieh, W. L., Chiou, S. H., & Kao, C. L. (2010). Ageing and neurodegenerative diseases. *Ageing Research Reviews*, *9*(Suppl 1), S36–S46. https://doi.org/10.1016/j.arr.2010.08.006

Ilic, K., Auer, B., Mlinac-Jerkovic, K., & Herrera-Molina, R. (2019). Neuronal signaling by Thy-1 in nanodomains with specific ganglioside composition: Shall we open the door to a new complexity? *Frontiers in Cell and Developmental Biology*, *7*, 27. https://doi.org/10.3389/fcell.2019.00027

Izquierdo, I., Quillfeldt, J. A., Zanatta, M. S., Quevedo, J., Schaeffer, E., Schmitz, P. K., & Medina, J. H. (1997). Sequential role of hippocampus and amygdala, entorhinal cortex and parietal cortex in formation and retrieval of memory for inhibitory avoidance in rats. *European Journal of Neuroscience*, *9*(4), 786–793. https://doi.org/10.1111/j.1460-9568.1997.tb01427.x

Jeyakumar, M., Thomas, R., Elliot-Smith, E., Smith, D. A., van der Spoel, A. C., d'Azzo, A., & Platt, F. M. (2003). Central nervous system inflammation is a hallmark of pathogenesis in mouse models of GM1 and GM2 gangliosidosis. *Brain*, *126*(Pt 4), 974–987. https://doi.org/10.1093/brain/awg089

Kallarackal, A. J., Kvarta, M. D., Cammarata, E., Jaberi, L., Cai, X., Bailey, A. M., & Thompson, S. M. (2013). Chronic stress induces a selective decrease in AMPA receptor-mediated synaptic excitation at hippocampal temporoammonic-CA1 synapses. *The Journal of Neuroscience*, *33*(40), 15669–15674. https://doi.org/10.1523/JNEUROSCI.2588-13.2013

Kim, J. J., & Diamond, D. M. (2002). The stressed hippocampus, synaptic plasticity and lost memories. *Nature Reviews Neuroscience*, *3*(6), 453–462. https://doi.org/10.1038/nrn849

Kolyovska, V. (2016). Serum IgG antibodies to GD1a and GM1 gangliosides in elderly people. *Biomeditsinskaya Khimiya*, *62*(1), 93–95. https://doi.org/10.18097/pbmc20166201093

Kuipers, S. D., Trentani, A., Den Boer, J. A., & Ter Horst, G. J. (2003). Molecular correlates of impaired prefrontal plasticity in response to chronic stress. *Journal of Neurochemistry*, *85*(5), 1312–1323. https://doi.org/10.1046/j.1471-4159.2003.01770.x

Lahiri, D. K. (2004). Functional characterization of amyloid beta precursor protein regulatory elements: Rationale for the identification of genetic polymorphism. *Annals of the New York Academy of Sciences*, *1030*, 282–288. https://doi.org/10.1196/annals.1329.035

Lovick, T. A. (2012). Estrous cycle and stress: Influence of progesterone on the female brain. *Brazilian Journal of Medical and Biological Research*, *45*, 314–320. https://doi.org/10.1590/S0100-879X2012007500044

Luine, V., Villegas, M., Martinez, C., & McEwen, B. S. (1994). Repeated stress causes reversible impairments of spatial memory performance. *Brain Research*, *639*(1), 167–170. https://doi.org/10.1016/0006-8993(94)91778-7

Lyons, C. E., & Bartolomucci, A. (2020). Stress and Alzheimer's disease: A senescence link? *Neuroscience & Biobehavioral Reviews*, *115*, 285–298. https://doi.org/10.1016/j.neubiorev.2020.05.010

Marin, R., & Diaz, M. (2018). Estrogen interactions with lipid rafts related to neuroprotection. Impact of brain ageing and menopause. *Frontiers in Neuroscience*, *12*, 128. https://doi.org/10.3389/fnins.2018.00128

Marzban, H., Khanzada, U., Shabir, S., Hawkes, R., Langnaese, K., Smalla, K.-H., Bockers, T. M., Gundelfinger, E. D., Gordon-Weeks, P. R., & Beesley, P. W. (2003). Expression of the immunoglobulin superfamily neuroplastin adhesion molecules in adult and developing mouse cerebellum and their localisation to parasagittal stripes. *The Journal of Comparative Neurology*, *462*, 286–301. https://doi.org/10.1002/cne.10719

Mesa-Herrera, F., Taoro-González, L., Valdés-Baizabal, C., Diaz, M., & Marín, R. (2019). Lipid and lipid raft alteration in aging and neurodegenerative diseases: A window for the development of new biomarkers. *International Journal of Molecular Sciences*, *20*(15), 3810. https://doi.org/10.3390/ijms20153810

Miyagi, T., & Yamaguchi, K. (2012). Mammalian sialidases: Physiological and pathological roles in cellular functions. *Glycobiology*, *22*(7), 880–896. https://doi.org/10.1093/glycob/cws057

Owczarek, S., Soroka, V., Kiryushko, D., Larsen, M. H., Yuan, Q., Sandi, C., Berezin, V., & Bock, E. (2011). Neuroplastin-65 and a mimetic peptide derived from its homophilic binding site modulate neuritogenesis and neuronal plasticity. *Journal of Neurochemistry*, *117*(6), 984–994. https://doi.org/10.1111/j.1471-4159.2011.07269.x

Palpagama, T. H., Waldvogel, H. J., Faull, R. L. M., & Kwakowsky, A. (2019). The role of microglia and astrocytes in Huntington's disease. *Frontiers in Molecular Neuroscience*, *12*, 258. https://doi.org/10.3389/fnmol.2019.00258

Pavel, M. A., Petersen, E. N., Wang, H., Lerner, R. A., & Hansen, S. B. (2020). Studies on the mechanism of general anesthesia. *Proceedings*

of the National Academy of Sciences of the United States of America, *117*(24), 13757–13766. https://doi.org/10.1073/pnas.2004259117

Prendergast, J., Umanah, G. K. E., Yoo, S.-W., Lagerlof, O., Motari, M. G., Cole, R. N., Huganir, R. L., Dawson, T. M., Dawson, V. L., & Schnaar, R. L. (2014). Ganglioside regulation of AMPA receptor trafficking. *The Journal of Neuroscience*, *34*(39), 13246–13258. https://doi.org/10.1523/JNEUROSCI.1149-14.2014

Rossi, D., & Volterra, A. (2009). Astrocytic dysfunction: Insights on the role in neurodegeneration. *Brain Research Bulletin*, *80*(4–5), 224–232. https://doi.org/10.1016/j.brainresbull.2009.07.012

Sambamurti, K., Kinsey, R., Maloney, B., Ge, Y. W., & Lahiri, D. K. (2004). Gene structure and organization of the human beta-secretase (BACE) promoter. *The FASEB Journal*, *18*(9), 1034–1036. https://doi.org/10.1096/fj.03-1378fje

Sandi, C. (2004). Stress, cognitive impairment and cell adhesion molecules. *Nature Reviews Neuroscience*, *5*, 917. https://doi.org/10.1038/nrn1555

Schindelin, J., Arganda-Carreras, I., Frise, E., Kaynig, V., Longair, M., Pietzsch, T., Preibisch, S., Rueden, C., Saalfeld, S., Schmid, B., Tinevez, J.-Y., White, D. J., Hartenstein, V., Eliceiri, K., Tomancak, P., & Cardona, A. (2012). Fiji: An open-source platform for biological-image analysis. *Nature Methods*, *9*(7), 676–682. https://doi.org/10.1038/nmeth.2019

Schnaar, R. L., Gerardy-Schahn, R., & Hildebrandt, H. (2014). Sialic acids in the brain: Gangliosides and polysialic acid in nervous system development, stability, disease, and regeneration. *Physiological Reviews*, *94*(2), 461–518. https://doi.org/10.1152/physrev.00033.2013

Simons, K., & Toomre, D. (2000). Lipid rafts and signal transduction. *Nature Reviews Molecular Cell Biology*, *1*(1), 31–39. https://doi.org/10.1038/35036052

Smalla, K.-H., Matthies, H., Langnase, K., Shabir, S., Bockers, T. M., Wyneken, U., Staak, S., Krug, M., Beesley, P. W., & Gundelfinger, E. D. (2000). The synaptic glycoprotein neuroplastin is involved in long-term potentiation at hippocampal CA1 synapses. *Proceedings of the National Academy of Sciences of the United States of America*, *97*(8), 4327–4332. https://doi.org/10.1073/pnas.080389297

Sonnino, S., Chigorno, V., Aureli, M., Masilamani, A. P., Valsecchi, M., Loberto, N., & Prinetti, A. (2011). Role of gangliosides and plasma membrane-associated sialidase in the process of cell membrane organization. *Advances in Experimental Medicine and Biology*, *705*, 297–316. https://doi.org/10.1007/978-1-4419-7877-6_14

Soontornniyomkij, V., Risbrough, V. B., Young, J. W., Wallace, C. K., Soontornniyomkij, B., Jeste, D. V., & Achim, C. L. (2010). Short-term recognition memory impairment is associated with decreased expression of FK506 binding protein 51 in the aged mouse brain. *AGE*, *32*(3), 309–322. https://doi.org/10.1007/s11357-010-9145-9

Svennerholm, L. (1994). Ganglioside loss is a primary event in Alzheimer disease type I. *Progress in Brain Research*, *101*, 391–404. https://doi.org/10.1016/s0079-6123(08)61965-2

Svennerholm, L., Bostrom, K., Fredman, P., Mansson, J. E., Rosengren, B., & Rynmark, B. M. (1989). Human brain gangliosides: Developmental changes from early fetal stage to advanced age. *Biochimica Et Biophysica Acta*, *1005*(2), 109–117. https://doi.org/10.1016/0005-2760(89)90175-6

Vajn, K., Viljetic, B., Degmecic, I. V., Schnaar, R. L., & Heffer, M. (2013). Differential distribution of major brain gangliosides in the adult mouse central nervous system. *PLoS One*, *8*(9), e75720. https://doi.org/10.1371/journal.pone.0075720

Walker, F. R., Nilsson, M., & Jones, K. (2013). Acute and chronic stress-induced disturbances of microglial plasticity, phenotype and function. *Current Drug Targets*, *14*(11), 1262–1276. https://doi.org/10.2174/13894501131499990208

Wang, Y., Li, M., Tang, J., Song, M., Xu, X., Xiong, J., Li, J., & Bai, Y. (2011). Glucocorticoids facilitate astrocytic amyloid-β peptide deposition by increasing the expression of APP and BACE1 and decreasing the expression of amyloid-β-degrading proteases. *Endocrinology*, *152*(7), 2704–2715. https://doi.org/10.1210/en.2011-0145

Williamson, J. M., & Lyons, D. A. (2018). Myelin dynamics throughout life: An ever-changing landscape? *Frontiers in Cellular Neuroscience*, *12*, 424. https://doi.org/10.3389/fncel.2018.00424

Woo, H., Hong, C. J., Jung, S., Choe, S., & Yu, S.-W. (2018). Chronic restraint stress induces hippocampal memory deficits by impairing insulin signaling. *Molecular Brain*, *11*(1), 37. https://doi.org/10.1186/s13041-018-0381-8

Zárate, S., Stevnsner, T., & Gredilla, R. (2017). Role of estrogen and other sex hormones in brain aging. Neuroprotection and DNA repair. *Frontiers in Aging Neuroscience*, *9*, 430. https://doi.org/10.3389/fnagi.2017.00430

Zhang, P., Kishimoto, Y., Grammatikakis, I., Gottimukkala, K., Cutler, R. G., Zhang, S., Abdelmohsen, K., Bohr, V. A., Misra Sen, J., Gorospe, M., & Mattson, M. P. (2019). Senolytic therapy alleviates Aβ-associated oligodendrocyte progenitor cell senescence and cognitive deficits in an Alzheimer's disease model. *Nature Neuroscience*, *22*(5), 719–728. https://doi.org/10.1038/s41593-019-0372-9

Zhang, Y., Guo, O., Huo, Y., Wang, G., & Man, H.-Y. (2018). Amyloid-β induces AMPA receptor ubiquitination and degradation in primary neurons and human brains of Alzheimer's disease. *Journal of Alzheimer's Disease*, *62*(4), 1789–1801. https://doi.org/10.3233/JAD-170879

SUPPORTING INFORMATION

Additional supporting information may be found online in the Supporting Information section.

How to cite this article: Balog M, Blažetić S, Ivić V, et al. Disarranged neuroplastin environment upon aging and chronic stress recovery in female Sprague Dawley rats. *Eur J Neurosci*. 2022;55(9):2474–2490. https://doi.org/10.1111/ejn.15256